Supplementary figure legends

Figure 1—figure supplement 1. Loss of TCAs in *Gbx2* knock-out mice

Tracing of TCAs (arrowheads in top panels) after injection of DiI crystals in the dorsal thalamus at E16.5 (upper panels), prospective primary somatosensory (S1, middle panels) or visual (V1, lower panels) cortices of neonatal wild type (wt) and *Gbx2* knock-out (*Gbx2* ko) mice. Ic, internal capsule; DLG, dorsal lateral geniculate nucleus; VLG, ventrolateral geniculate nucleus; VPL, ventral posteriolateral thalamic nucleus. Scale bar 100µm.

Figure 1—figure supplement 2. Loss of TCAs in *Gbx2* knock-out mice does not affect neocortical layering at birth

Expression of cortical layer markers (Molyneaux et al., 2007) in prospective S1 cortex of newborn wild type (wt) and *Gbx2* knock-out mice.

A) In situ hybridization for *Cux1* (CX, a marker of layers II-IV, red) and *CTIP2* (CT, a marker of layer V, green) combined with immunohistochemistry for Tbr1 (Tb, a marker of layer VI, blue). Arrows denote unspecifically labeled blood vessels. IZ, intermediate zone. Scale bar, 50µm.

B) In situ hybridization for *RoRβ* (Rβ, a marker of layer IV, red), *CTIP2* (green) combined with immunohistochemistry for Tbr1 (blue). Scale bar, 50µm.

Figure 1—figure supplement 3. Loss of TCAs in *Gbx2* knock-out mice does not affect neocortical arealization

Neocortical arealization (sagittal views) in newborn wild type (wt) and *Gbx2* knock-out mice assessed by *in situ* hybridization for Lmo4 (A) and Cad8 (B). Arrowheads indicate borders between different areas. Fr, frontal cortex; Par, parietal cortex (prospective somatosensory cortex); Occ, occipital cortex (prospective visual cortex); Str, striatum; Hip, hippocampus; Scale bar, 250µm.

Figure 1—figure supplement 4. Schematic of upper, middle and lower frames used for quantification of laminar distribution of GABAergic interneurons in newborn mouse neocortex

In situ hybridization for *Cux1* (red, panel A) and *CTGF* (red, panel B) combined with immunohistochemistry for Tbr1 (blue) and *CTIP2* (green). Scale bar, 100μm. The upper frame encompassed layers II to V demarcated by the expression of Cux1 and CTIP2. The middle frame encompassed the majority of the Tbr1-positive territory between the CTIP2 and CTGF markers (layer VIa). The lower frame included layer VIb (or subplate) expressing CTGF and the underlying intermediate zone (IZ). Each frame was 150x600 μm in size, corresponding to an area of $9x10^4$ μm^2. Expression of *CTGF*, marking the subplate (layer VIb), was detected by *in situ* hybridization.

Figure 1—figure supplement 5. Normal proportion of GABAergic interneurons in superficial versus deep routes of tangential migration in *Gbx2* knock-out embryos

A) Lhx6-GFP^+ interneurons (green) in prospective somatosensory cortex of newborn wild type (wt) and *Gbx2* knock-out (ko) mice at E14.5 and E16.5 combined with immunostaining against CTIP2 (red). Arrow head indicate unspecifically labeled blood vessels above cortex. Scale bar, 50μm.

B) Quantification of Lhx6-GFP^+ interneurons in the marginal zone (MZ) and subventricular/intermediate zones (SVZ/IZ) in *Gbx2* knock-out and wild type embryos at E14.5 and E16.5. Results are expressed as average ± SEM (n.s., not significant [p>0.05]; N = 6 mice per group).

Figure 1—figure supplement 6. Lack of TCAs in *Gbx2* mutant mice affects the laminar distribution of different classes of MGE-derived interneurons to a similar extent

A) Relative distribution of BrdU•Lhx6-GFP double positive cells in upper and lower cortical layers of wild type (wt) and *Gbx2* knock-out E18.5 embryos injected with BrdU at E12.5 (left) or E14.5 (right). Results are expressed as average percentage ± SEM

relative to the total number of BrdU•Lhx6-GFP double positive cells counted (*, $p<0.05$, N=3 embryos in each group).

B) Satb1$^+$ (red) and Lhx6-GFP$^+$ (green) interneurons in prospective somatosensory cortex of newborn wild type (wt) and *Gbx2* knock-out (ko) mice. Scale bar 50µm.

C) Quantification of the percentage of Satb1$^+$ cells among Lhx6-GFP$^+$ interneurons in upper and lower cortical layers of wild type (wt) and *Gbx2* knock-out newborn mice. Results are expressed as average ± SEM (n.s., non-significant; N=3 mice).

Figure 2—figure supplement 1. Fate mapping of Olig3$^+$ E10.5 precursors at P0 and P21

dTomato expression in brains of *Olig3-Cre*^{ERT2};*dTom* mice at P0 (A) or P21 (B) after tamoxifen administration at E10.5. Show are fluorescent micrographs of coronal sections taken at the level of the thalamus (a), visual cortex (b) and thalamic sensory and visual projection nuclei (c). RSG, retrosplenial granular cortex; M1, primary motorcortex; S1, primary somatosensory cortex; S2, secondary somatosensory cortex; V1, primary visual cortex; V2M, secondary medial visual cortex; V2L, secondary lateral visual cortex; Hip, hippocampus; Au, auditory cortex; Pir, piriform cortex; MGV, medial geniculate nucleus; SC, superior colliculus, SN, substantia nigra; DLG, dorsal lateral geniculate nucleus; VLG, ventrolateral geniculate nucleus; VPL, ventral posterolateral thalamic nucleus; VPM, ventral posteromedial thalamic nucleus. Scale bars, 500µm (a) and 100µm (b and c).

Figure 2—figure supplement 2. Verification of removal of *Gbx2* expression in the thalamus of *Gbx2* mutant mice

In situ hybridization for *Gbx2* in wild type (wt) and *Gbx2* knock-out (*Gbx2* ko) mice (A) and in *Gbx2*$^{fx/fx}$ and *Olig3-Cre*^{ERT2};*Gbx2*$^{fx/fx}$ conditional mutant mice (B) at E12.5. Conditional mutant embryos received tamoxifen at E10.5, causing significant reduction of *Gbx2* expression. ET, epithalamus; THne, intermediate thalamic neuroepithelium; THdz, intermediate thalamic differentiating zone; HT, hypothalamus; Scale bar, 100µm.

Figure 2—figure supplement 3. Loss of TCAs in *Olig3-Cre*^{ERT2};*Gbx2*$^{fx/fx}$ conditional mutant mice

Tracing of TCAs (arrowheads in top panels) after injection of DiI crystals in dorsal thalamus at E16.5 (upper panels), prospective primary somatosensory (S1, middle panels) or visual (V1, lower panels) cortices of neonatal *Gbx2*$^{fx/fx}$ controls and *Olig3-Cre*^{ERT2};*Gbx2*$^{fx/fx}$ conditional mutant mice. Note the absence of DiI staining in ventral posterolateral nucleus (VPL) of conditional mutant after S1 injection and in the lateral geniculate nucleus (DLG and VLG) after V1 injection. ic, internal capsule; DLG, dorsal lateral geniculate nucleus; VLG, ventral lateral geniculate nucleus. Scale bar 200µm.

Figure 2—figure supplement 4. Fate mapping of Gbx2^{+} precursor cells

Coronal section of *Gbx2-Cre*^{ERT2};*dTom* P21 brain (A) after tamoxifen injection at E10.5 showing cell bodies in thalamic nuclei (lower inset, B) and axonal projections in cortex barrel fields of S1 (upper inset, C). Note the absence of labeled neuronal cell bodies in S1 neocortex (C), indicating lack of contribution of embryonic Gbx2-expressing precursors to the postnatal neocortex. Cpu, caudate-putamen; DLG, dorsal lateral geniculate nucleus; Hip, hippocampus; S1, primary somatosensory cortex; S1BF: barrel field of primary somatosensory cortex; S2: secondary somatosensory cortex; VPM, ventral posteromedial thalamic nucleus; VPL, ventral posterolateral thalamic nucleus; I-VI, layer I-VI; IZ, intermediate zone; Scale bars A, 500µm; B, C, 100µm.

Figure 6—figure supplement 1. Absence of VGLUT1 expression in TCAs of *Olig3-Cre*^{ERT2};*Vglut2*$^{\Delta/fx}$ conditional mutant mice

Immunohistochemistry for VGLUT1 (green) and 5HTT (red) in prospective S1 cortex of wild type (*Vglut2*$^{+/+}$) and *Olig3-Cre*^{ERT2};*Vglut2*$^{\Delta/fx}$ conditional mutant mice. VGLUT1 expression remained undetectable in TCAs lacking VGLUT2. Scale bar 100µm.

Figure 7—figure supplement 1. Knock-down of NMDA receptor subunit NR2B in GABAergic interneurons by *in utero* electroporation

Analysis of NR2B expression in cultured GABAergic interneurons dissociated from the MGE of embryos subjected to *in utero* electroporation. Immunocytochemistry for NR2B is shown in blue. RFP (red) marks all electroporated neurons. EGFP (green) expressed under the Dlx5/6 promoter marks electroporated GABAergic interneurons. Note the loss of NR2B immunoreactivity in neurons electroporated with shNR2B but not in neurons that received control shRNA or in non-electroporated cells. Scale bar 50µm.

Figure 9—figure supplement 1. Abnormal laminar distribution of cortical GABAergic interneurons in newborn *Olig3-Cre*;*Gbx2*$^{fx/fx}$ mice

A) Immunostaining for Lhx6 (green), CTIP2 (red) and Tbr1 (blue) in prospective visual cortex of newborn *Olig3-Cre;Gbx2*$^{fx/fx}$ conditional mutant and *Gbx2*$^{fx/fx}$ control mice. Scale bar, 100µm.

B-C) Quantification of Lhx6^{+} interneurons in upper (B) and lower (C) layers of prospective primary motor (M1), somatosensory (S1), and visual (V1) cortices of newborn *Olig3-Cre*;*Gbx2*$^{fx/fx}$ conditional mutant and *Gbx2*$^{fx/fx}$ control mice. Results are expressed as average ± SEM (*, $p<0.05$; **: $p<0.005$; N=3 mice per group).

Fig. 1

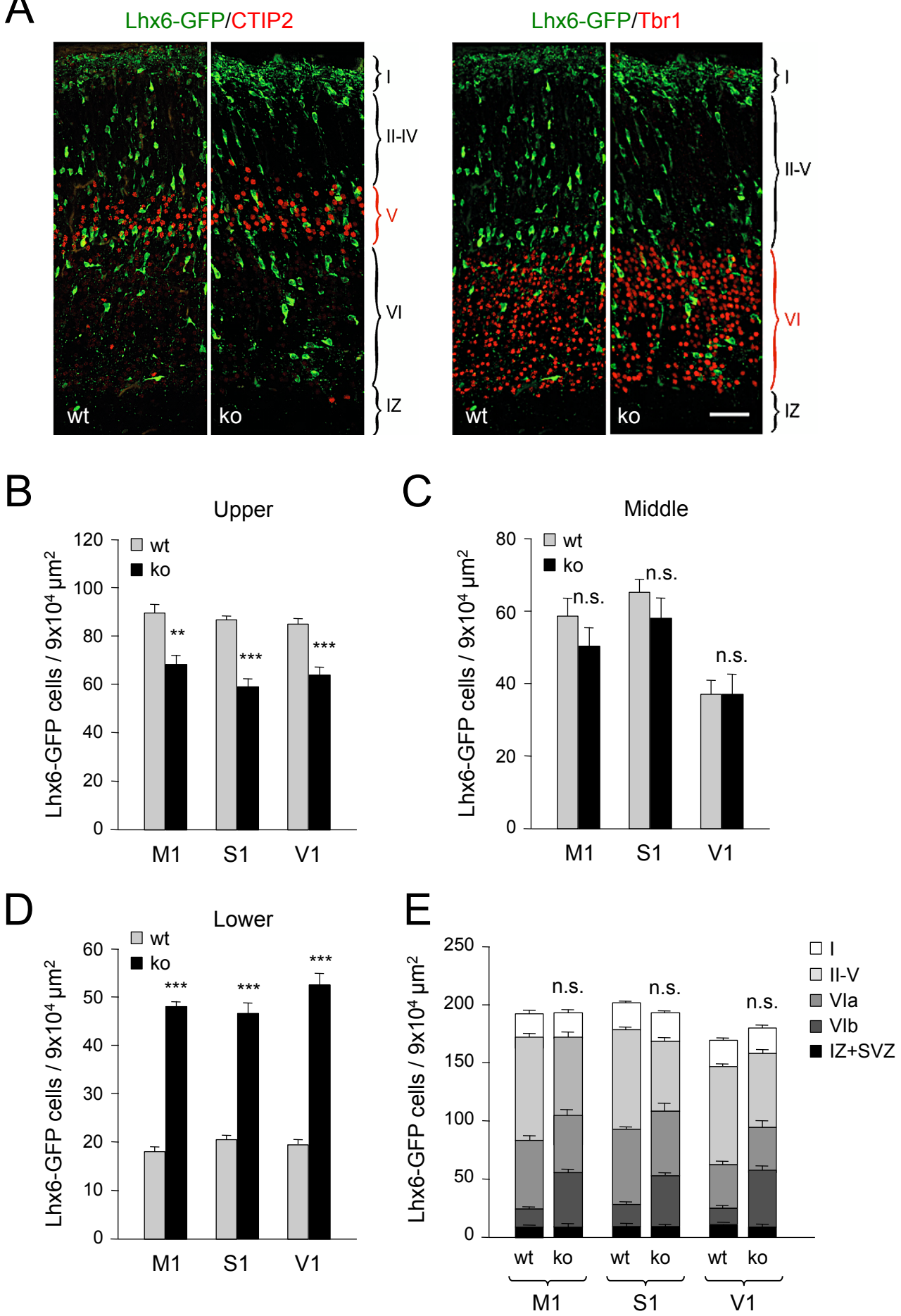
A
Lhx6-GFP/CTIP2
Lhx6-GFP/Tbr1
I
II-IV
V
VI
IZ
wt
ko
I
II-V
VI
IZ
wt
ko
B
Upper
Lhx6-GFP cells / 9x10⁴ µm²
wt
ko
**
***
***
M1
S1
V1
C
Middle
Lhx6-GFP cells / 9x10⁴ µm²
wt
ko
n.s.
n.s.
n.s.
M1
S1
V1
D
Lower
Lhx6-GFP cells / 9x10⁴ µm²
wt
ko
***
***
***
M1
S1
V1
E
Lhx6-GFP cells / 9x10⁴ µm²
I
II-V
VIa
VIb
IZ+SVZ
n.s.
n.s.
n.s.
wt
ko
wt
ko
wt
ko
M1
S1
V1

Fig. 2

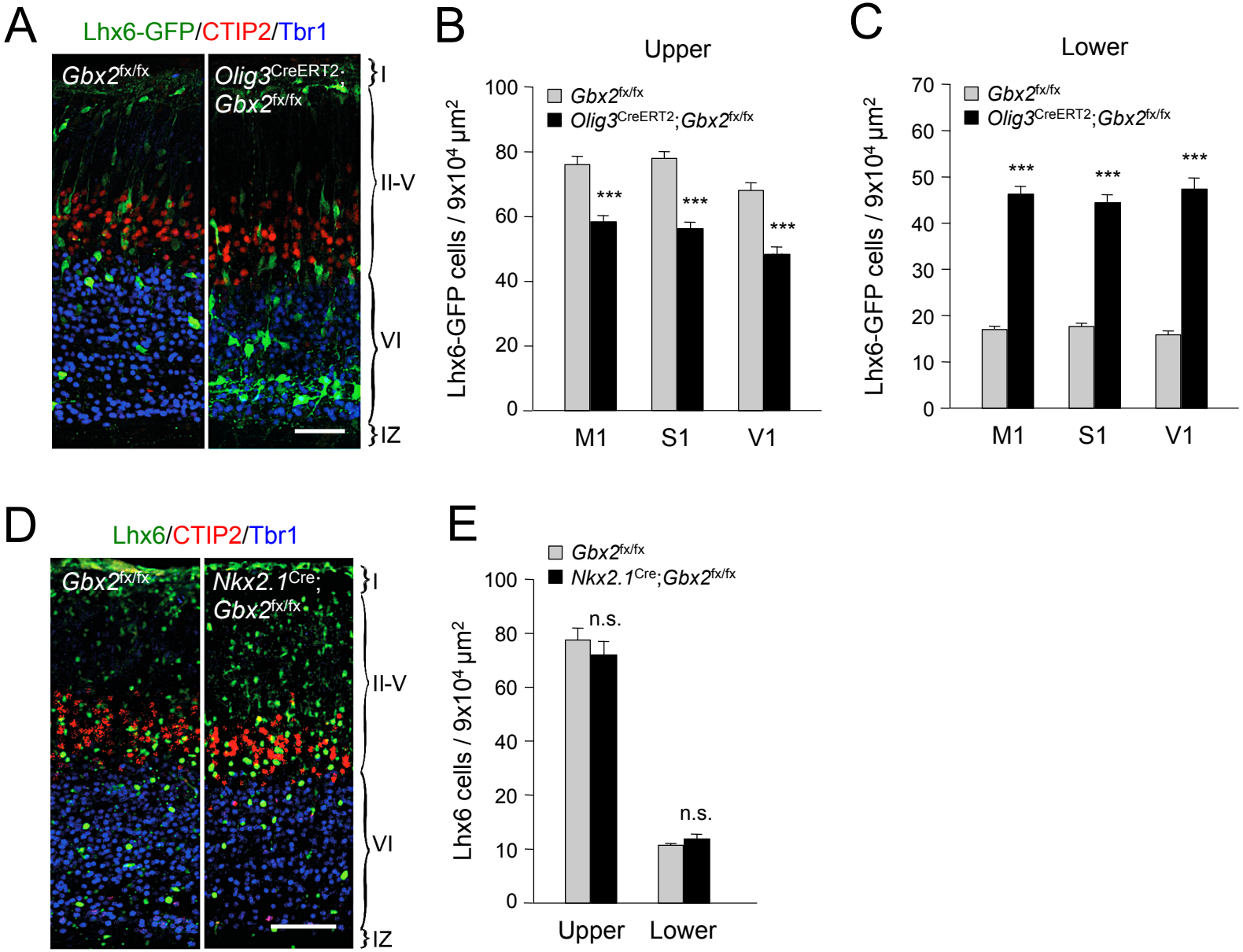
A
Lhx6-GFP/CTIP2/Tbr1
Gbx2fx/fx
Olig3CreERT2;
Gbx2fx/fx
I
II-V
VI
IZ
B
Upper
Gbx2fx/fx
Olig3CreERT2;Gbx2fx/fx
Lhx6-GFP cells / 9x10⁴ µm²
100
80
60
40
20
0
***
M1
S1
V1
C
Lower
70
60
50
40
30
20
10
0
D
Lhx6/CTIP2/Tbr1
Nkx2.1Cre;
Gbx2fx/fx
E
Nkx2.1Cre;Gbx2fx/fx
Lhx6 cells / 9x10⁴ µm²
n.s.
Upper
Lower

Fig. 3

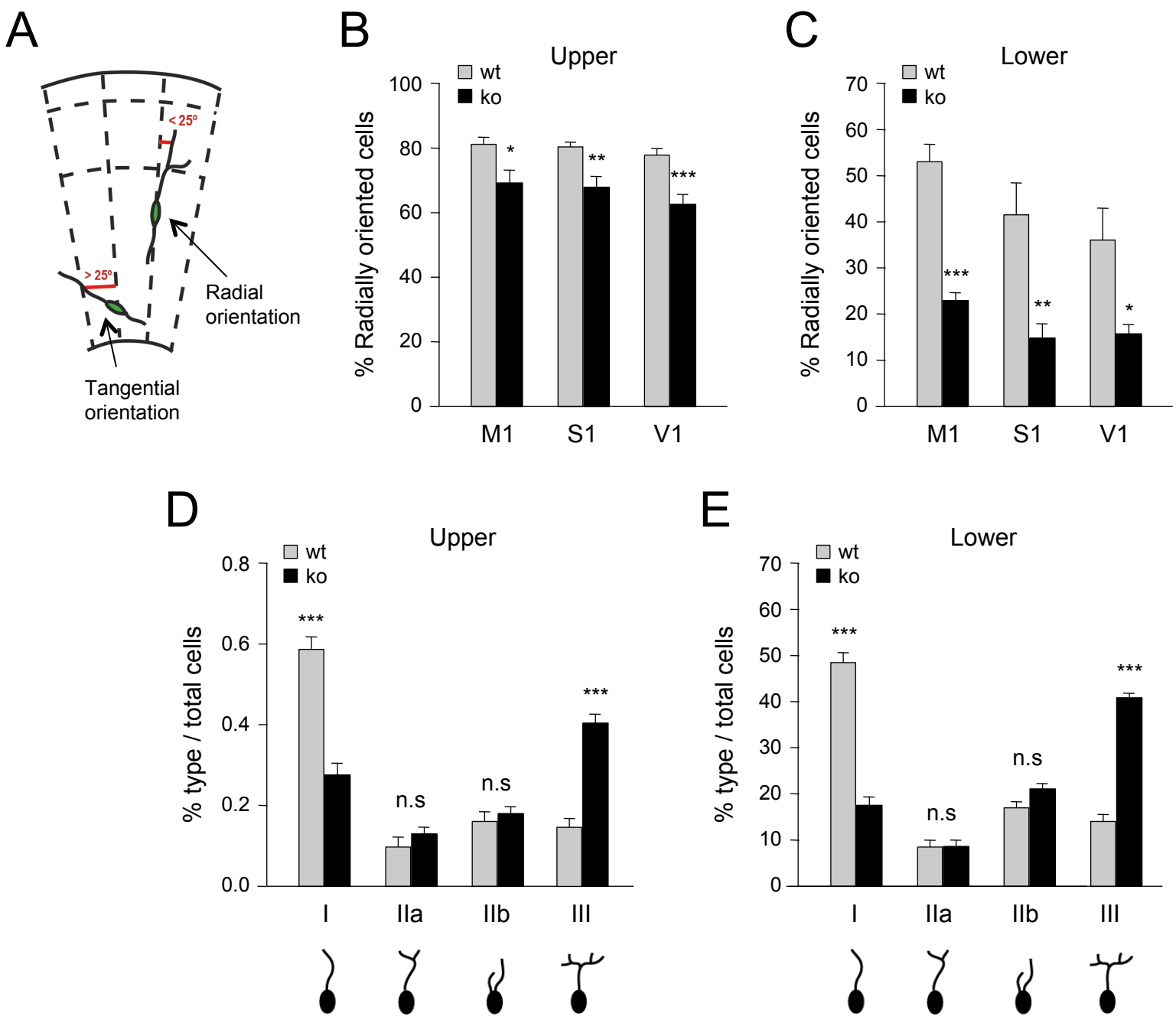
A
< 25º
> 25º
Radial orientation
Tangential orientation
B
Upper
wt
ko
% Radially oriented cells
100
80
60
40
20
0
*
**
***
M1
S1
V1
C
Lower
wt
ko
% Radially oriented cells
70
60
50
40
30
20
10
0
***
**
*
M1
S1
V1
D
Upper
wt
ko
% type / total cells
0.8
0.6
0.4
0.2
0.0
***
n.s
n.s
***
I
IIa
IIb
III
E
Lower
wt
ko
% type / total cells
70
60
50
40
30
20
10
0
***
n.s
n.s
***
I
IIa
IIb
III

Fig. 4

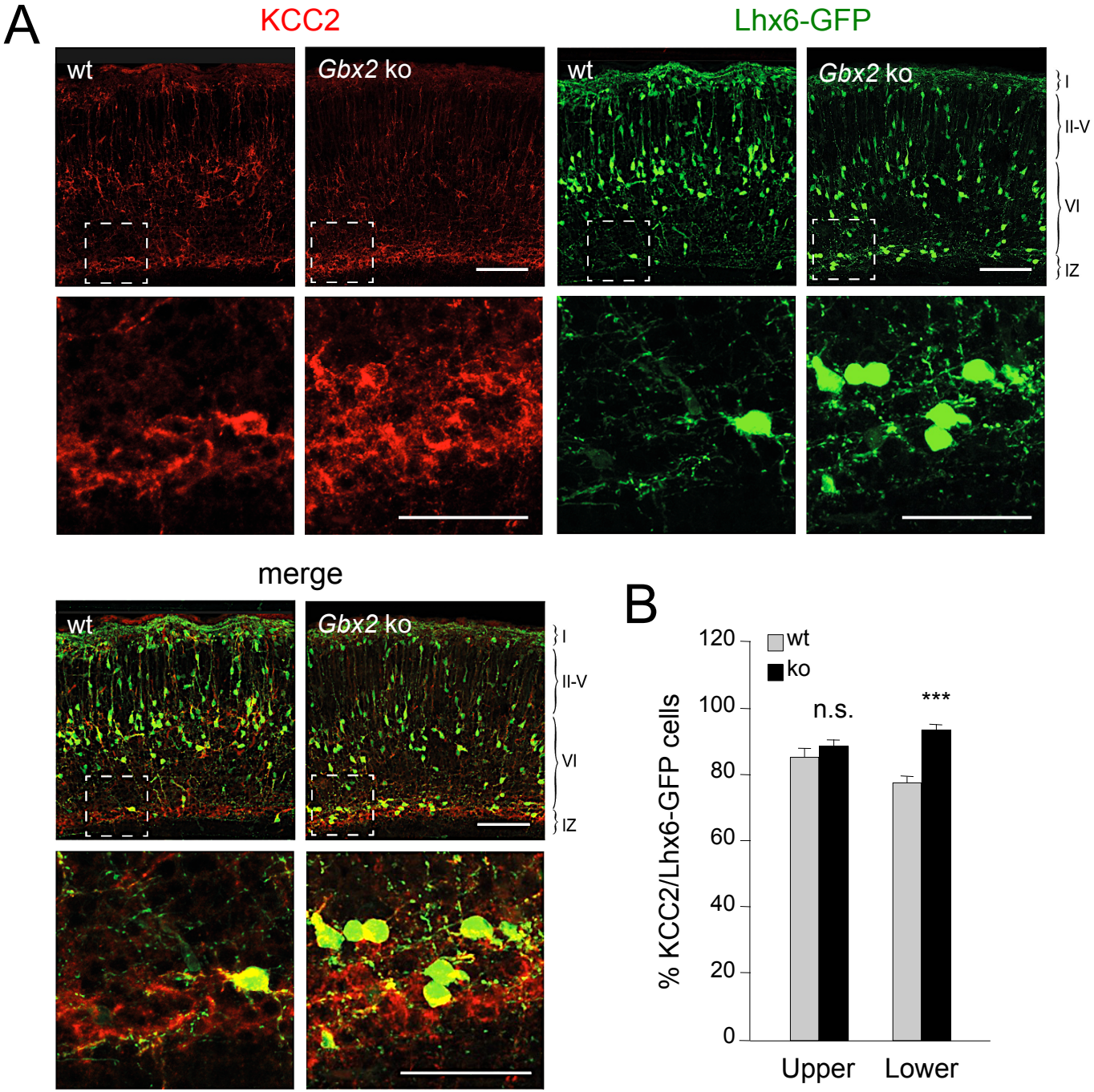
A
KCC2
Lhx6-GFP
wt
Gbx2 ko
wt
Gbx2 ko
I
II-V
VI
IZ
merge
wt
Gbx2 ko
I
II-V
VI
IZ
B
wt
ko
% KCC2/Lhx6-GFP cells
120
100
80
60
40
20
0
n.s.
***
Upper
Lower

Fig. 5

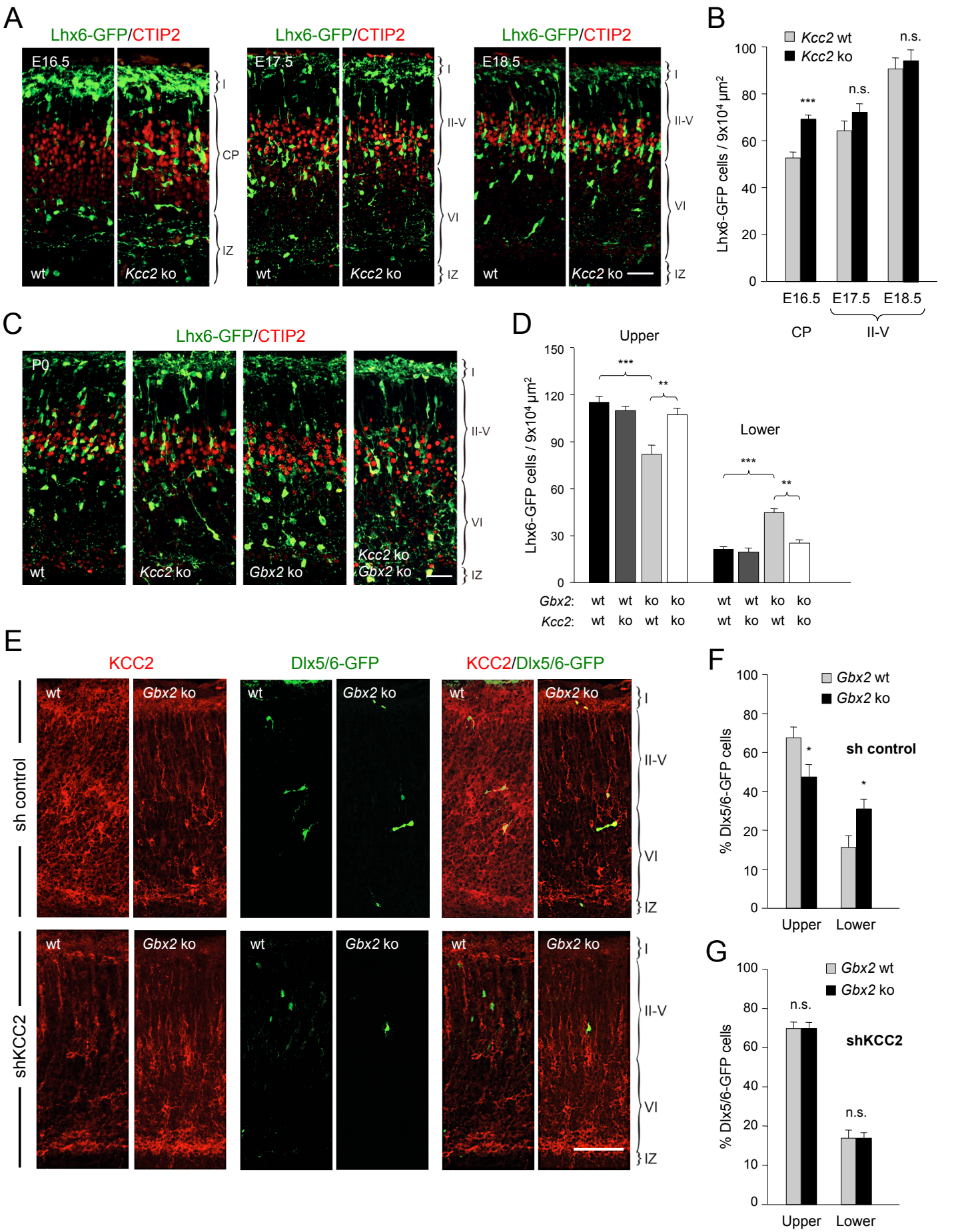
A
Lhx6-GFP/CTIP2
E16.5
E17.5
E18.5
wt
Kcc2 ko
I
CP
II-V
VI
IZ
B
Kcc2 wt
Kcc2 ko
Lhx6-GFP cells / 9x10⁴ µm²
n.s.
***
E16.5
E17.5
E18.5
CP
II-V
C
P0
Gbx2 ko
Kcc2 ko
Gbx2 ko
D
Upper
Lower
Gbx2:
Kcc2:
E
KCC2
Dlx5/6-GFP
KCC2/Dlx5/6-GFP
sh control
shKCC2
F
Gbx2 wt
Gbx2 ko
% Dlx5/6-GFP cells
sh control
Upper
Lower
G
shKCC2

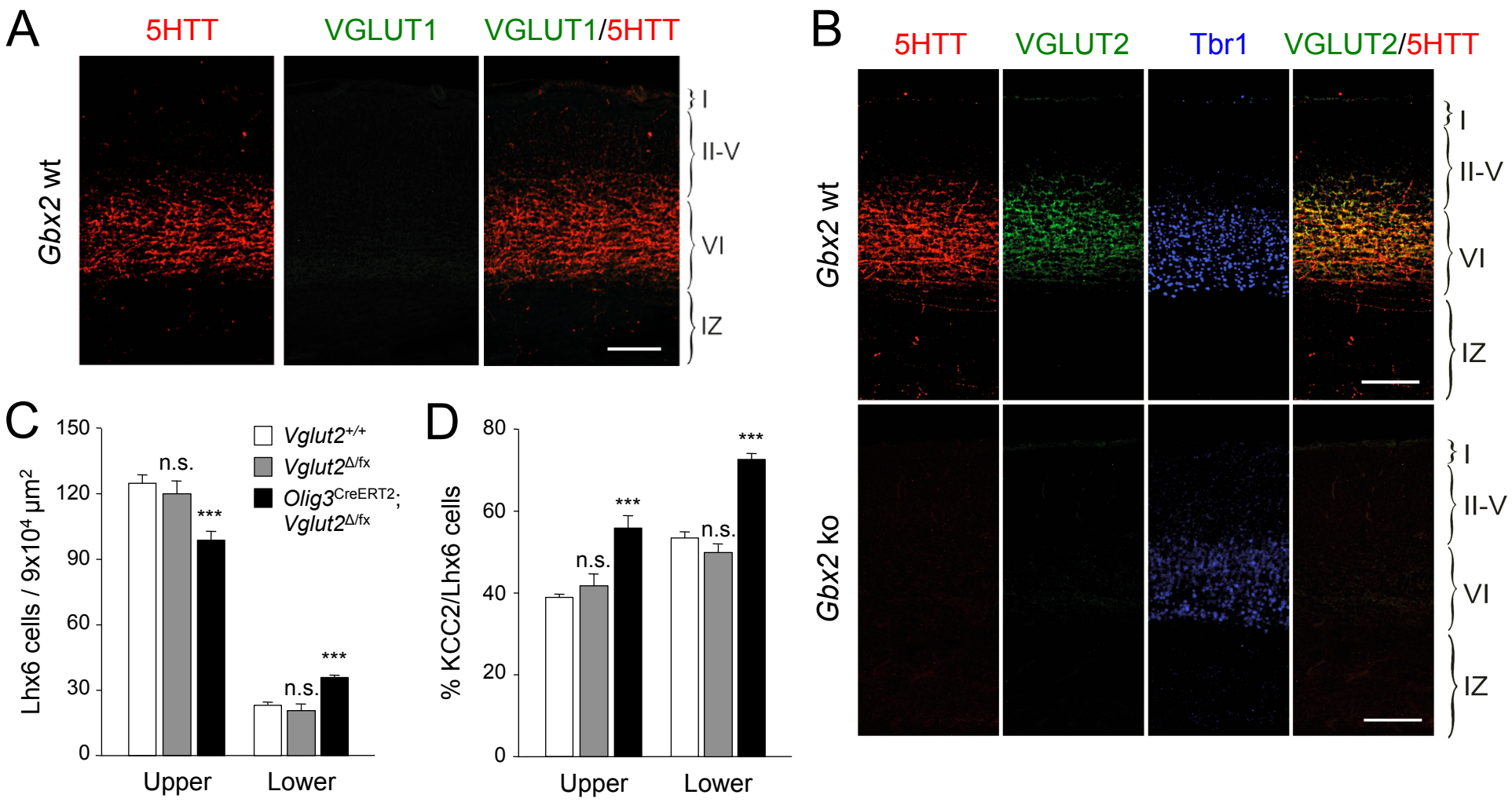
A
5HTT
VGLUT1
VGLUT1/5HTT
Gbx2 wt
I
II-V
VI
IZ
B
5HTT
VGLUT2
Tbr1
VGLUT2/5HTT
Gbx2 wt
Gbx2 ko
I
II-V
VI
IZ
C
Lhx6 cells / 9x10⁴ µm²
150
120
90
60
30
0
n.s.
***
n.s.
***
Vglut2+/+
Vglut2Δ/fx
Olig3CreERT2; Vglut2Δ/fx
Upper
Lower
D
% KCC2/Lhx6 cells
80
60
40
20
0
n.s.
***
n.s.
***
Upper
Lower

Fig. 7

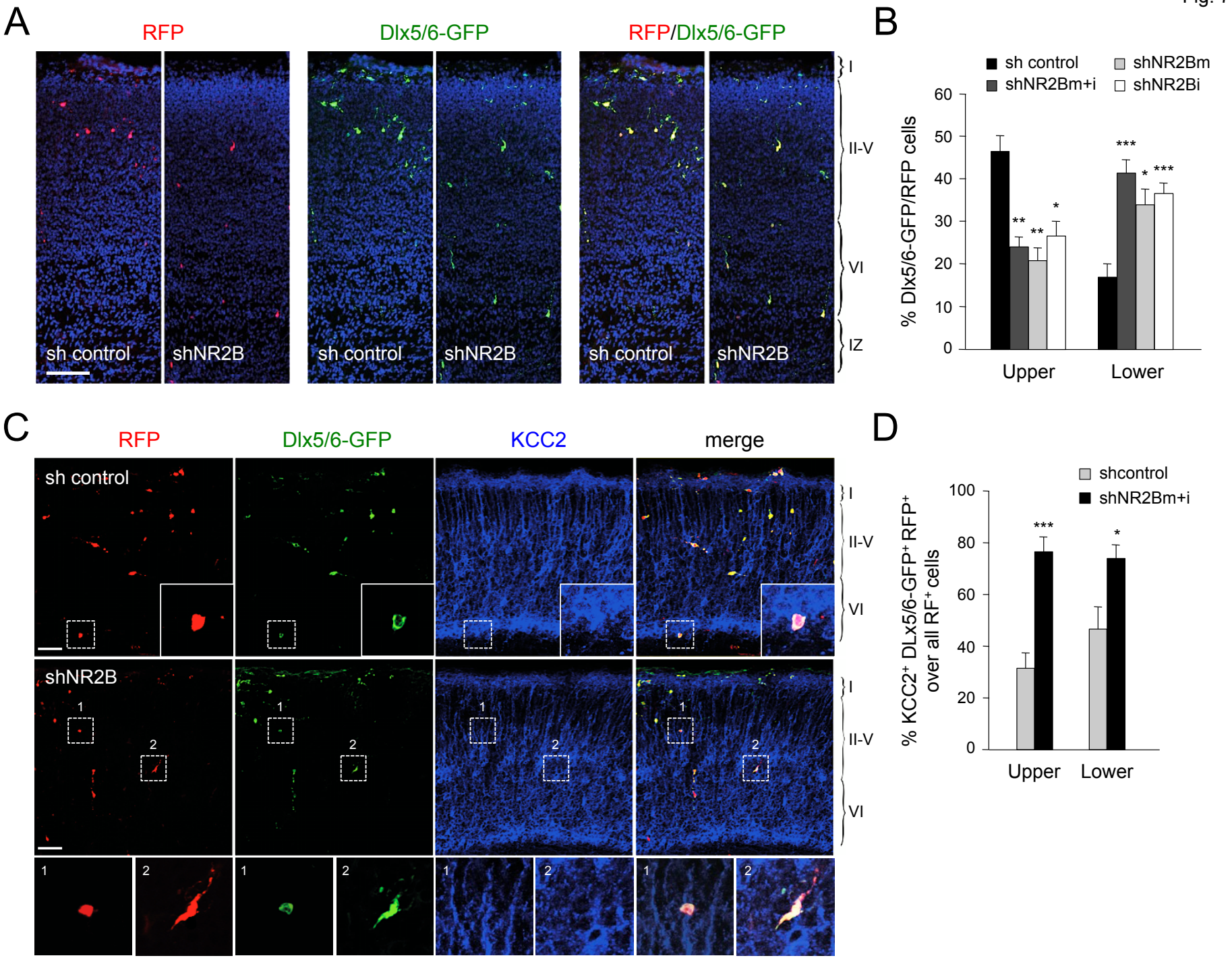
A
RFP
Dlx5/6-GFP
RFP/Dlx5/6-GFP
sh control
shNR2B
I
II-V
VI
IZ
B
sh control
shNR2Bm
shNR2Bm+i
shNR2Bi
% Dlx5/6-GFP/RFP cells
Upper
Lower
C
RFP
Dlx5/6-GFP
KCC2
merge
sh control
shNR2B
D
shcontrol
shNR2Bm+i
% KCC2+ DLx5/6-GFP+ RFP+ over all RF+ cells
Upper
Lower

Fig. 8

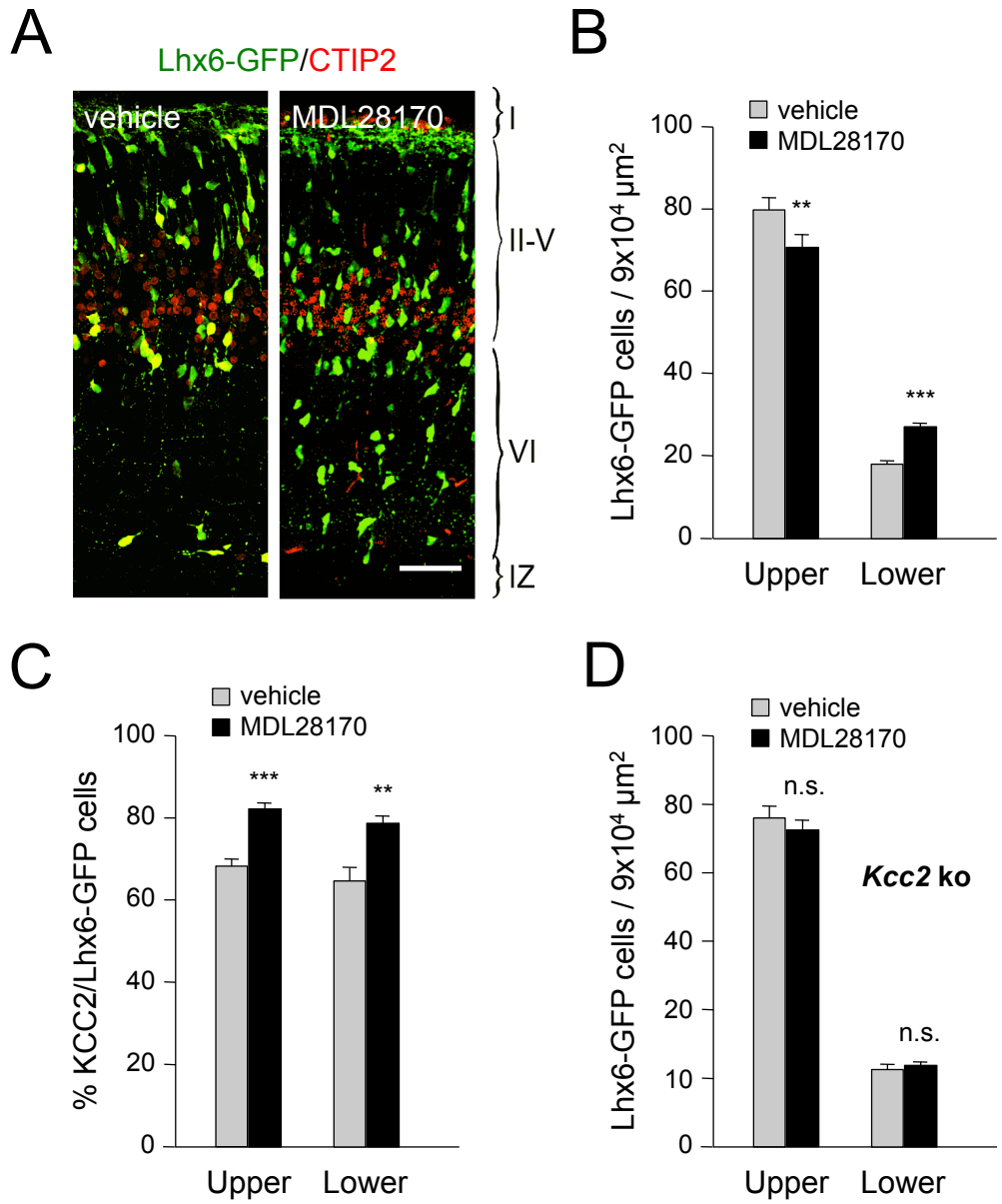
A
Lhx6-GFP/CTIP2
vehicle
MDL28170
I
II-V
VI
IZ
B
vehicle
MDL28170
Lhx6-GFP cells / 9x10⁴ µm²
100
80
60
40
20
0
**
***
Upper
Lower
C
vehicle
MDL28170
% KCC2/Lhx6-GFP cells
100
80
60
40
20
0
***
**
Upper
Lower
D
vehicle
MDL28170
Lhx6-GFP cells / 9x10⁴ µm²
100
80
60
40
20
10
0
n.s.
n.s.
Kcc2 ko
Upper
Lower

Fig. 9

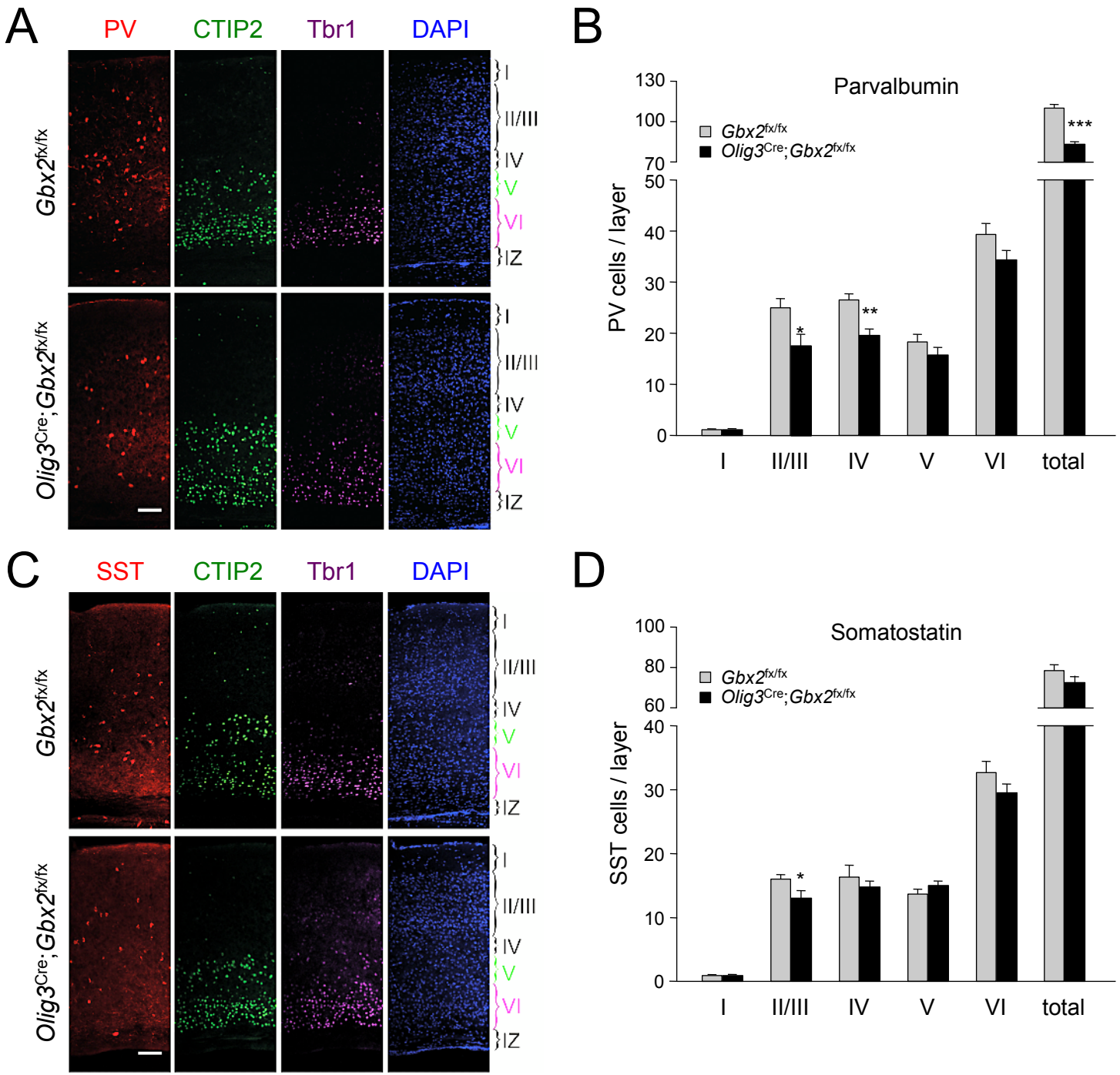
A
PV
CTIP2
Tbr1
DAPI
Gbx2fx/fx
Olig3Cre;Gbx2fx/fx
I
II/III
IV
V
VI
IZ
B
Parvalbumin
Gbx2fx/fx
Olig3Cre;Gbx2fx/fx
PV cells / layer
130
100
70
50
40
30
20
10
0
*
**
***
I
II/III
IV
V
VI
total
C
SST
CTIP2
Tbr1
DAPI
D
Somatostatin
SST cells / layer
100
80
60
40
30
20
10
0
*

Fig. 1S1

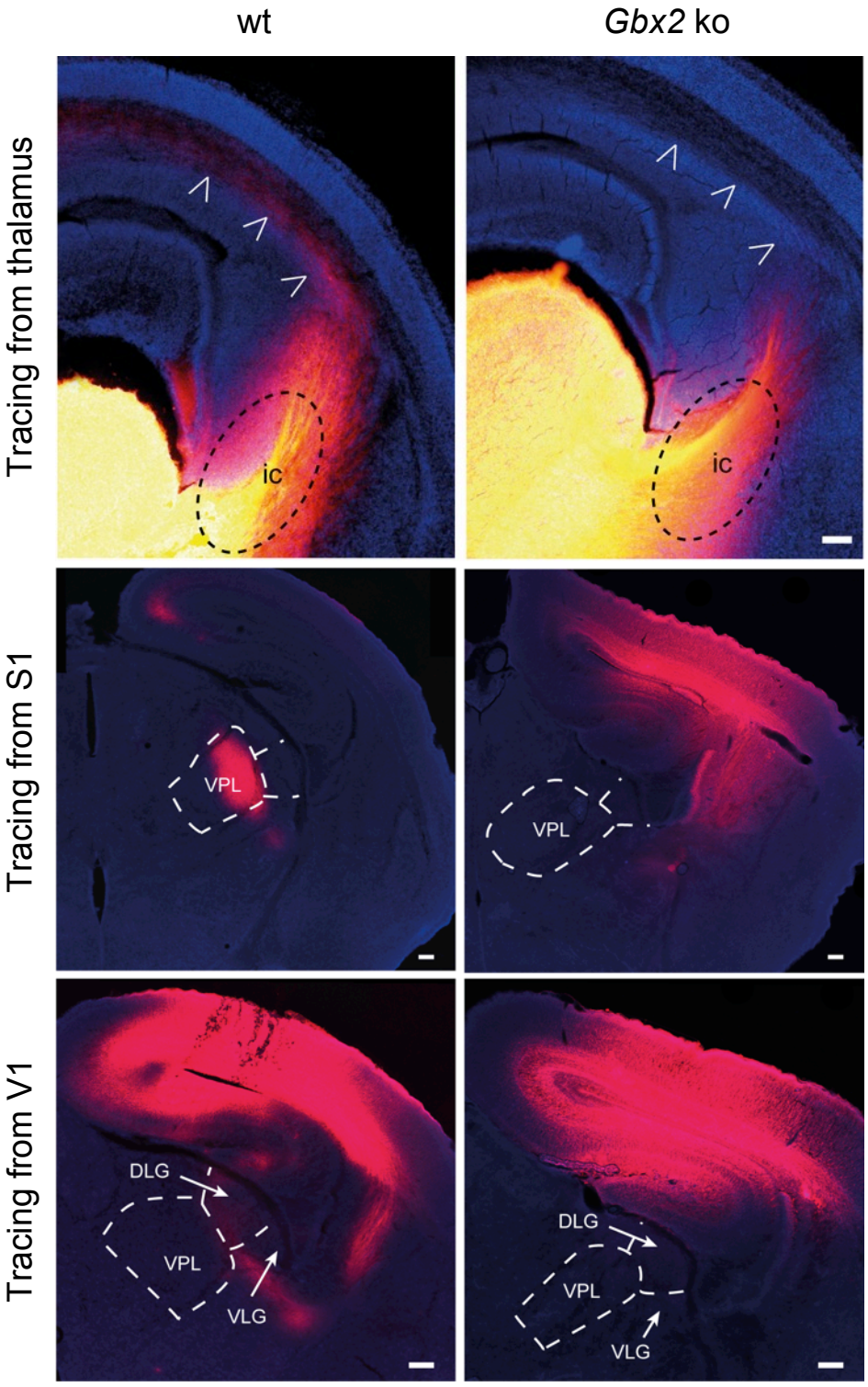
wt
Gbx2 ko
Tracing from thalamus
ic
ic
Tracing from S1
VPL
VPL
Tracing from V1
DLG
VPL
VLG
DLG
VPL
VLG

Fig. 1S2

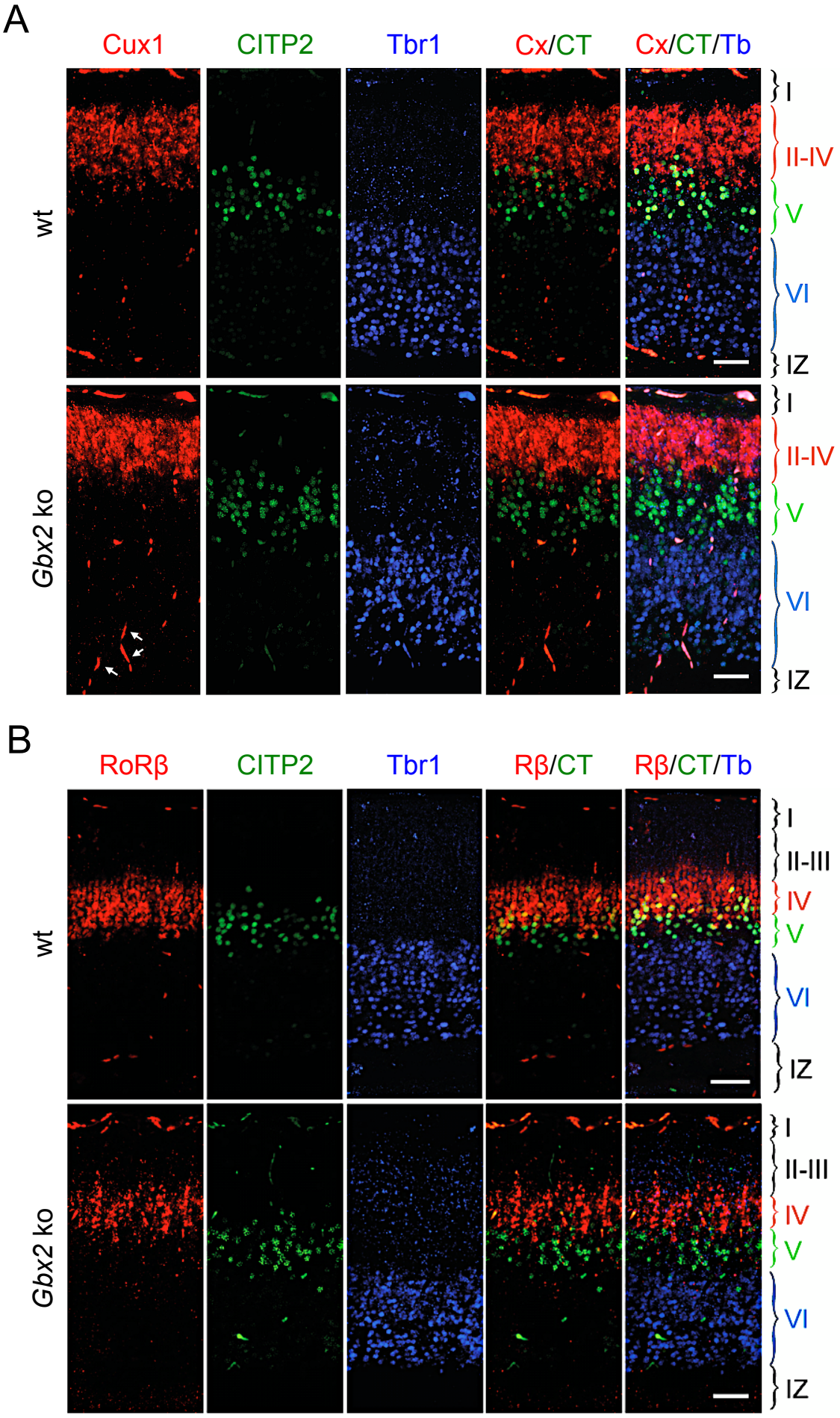
A
Cux1
CITP2
Tbr1
Cx/CT
Cx/CT/Tb
wt
Gbx2 ko
I
II-IV
V
VI
IZ
B
RoRβ
CITP2
Tbr1
Rβ/CT
Rβ/CT/Tb
wt
Gbx2 ko
I
II-III
IV
V
VI
IZ

Fig. 1S3

A

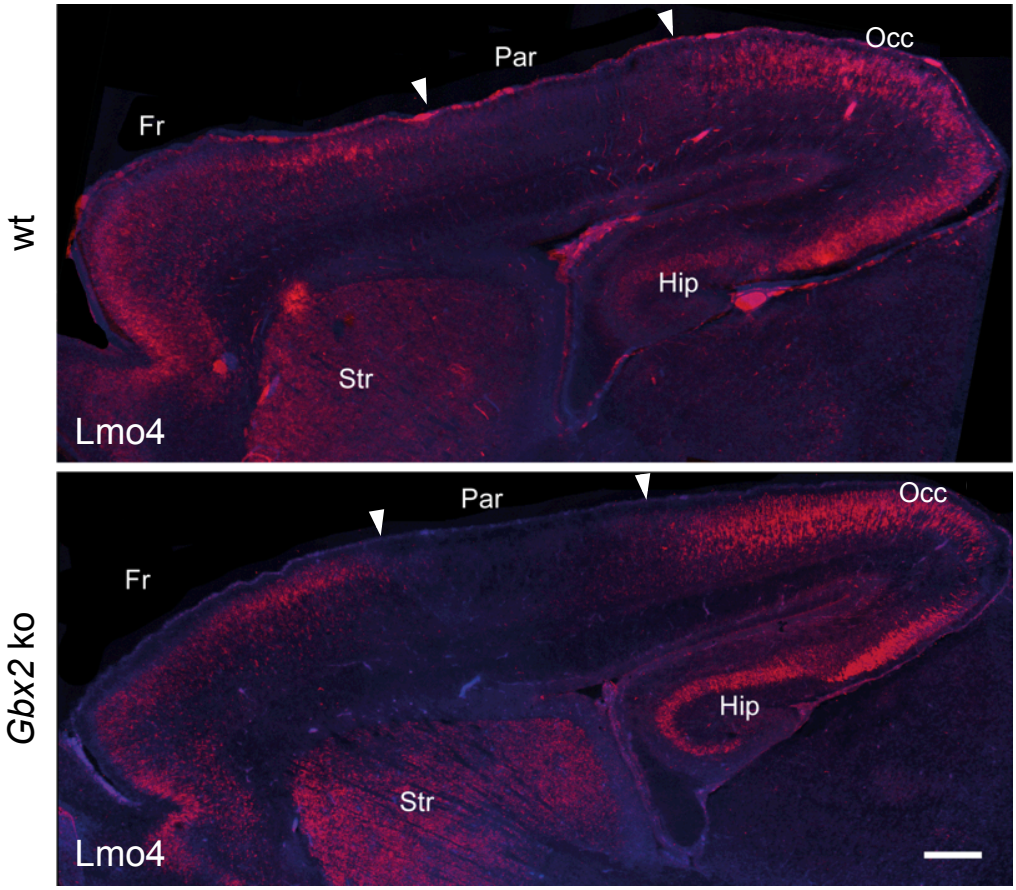
wt
Fr
Par
Occ
Hip
Str
Lmo4
Gbx2 ko
Fr
Par
Occ
Hip
Str
Lmo4

B

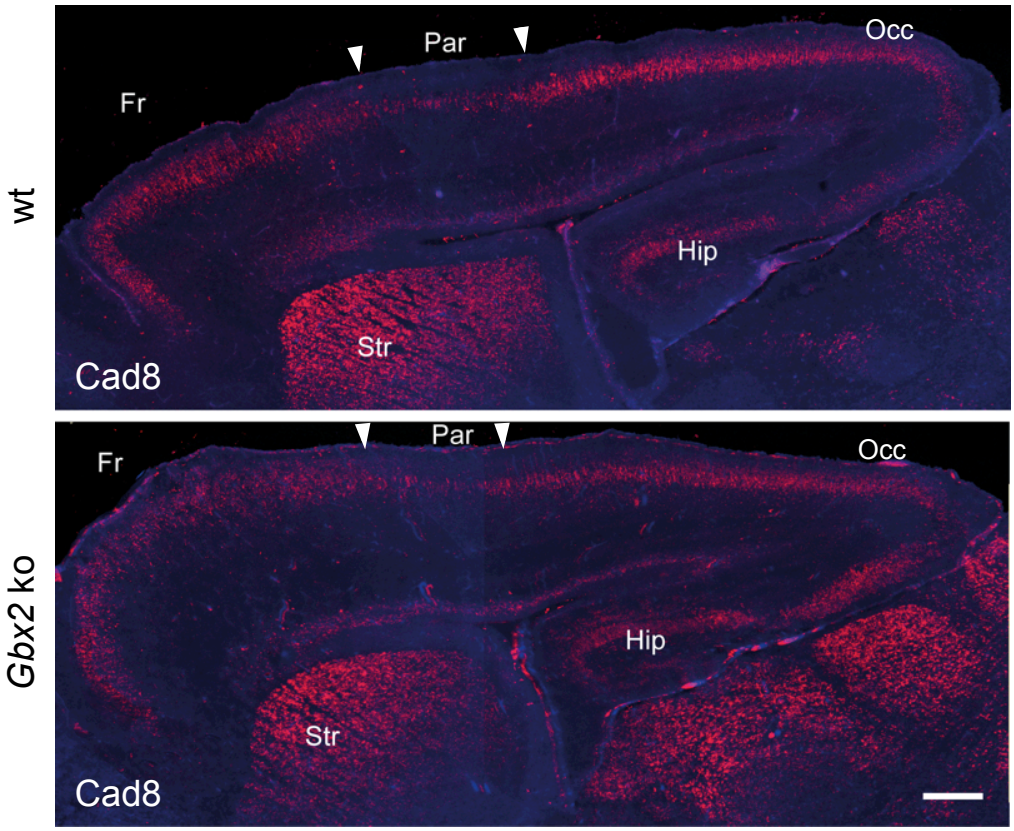
wt
Fr
Par
Occ
Hip
Str
Cad8
Gbx2 ko
Fr
Par
Occ
Hip
Str
Cad8

Fig. 1S4

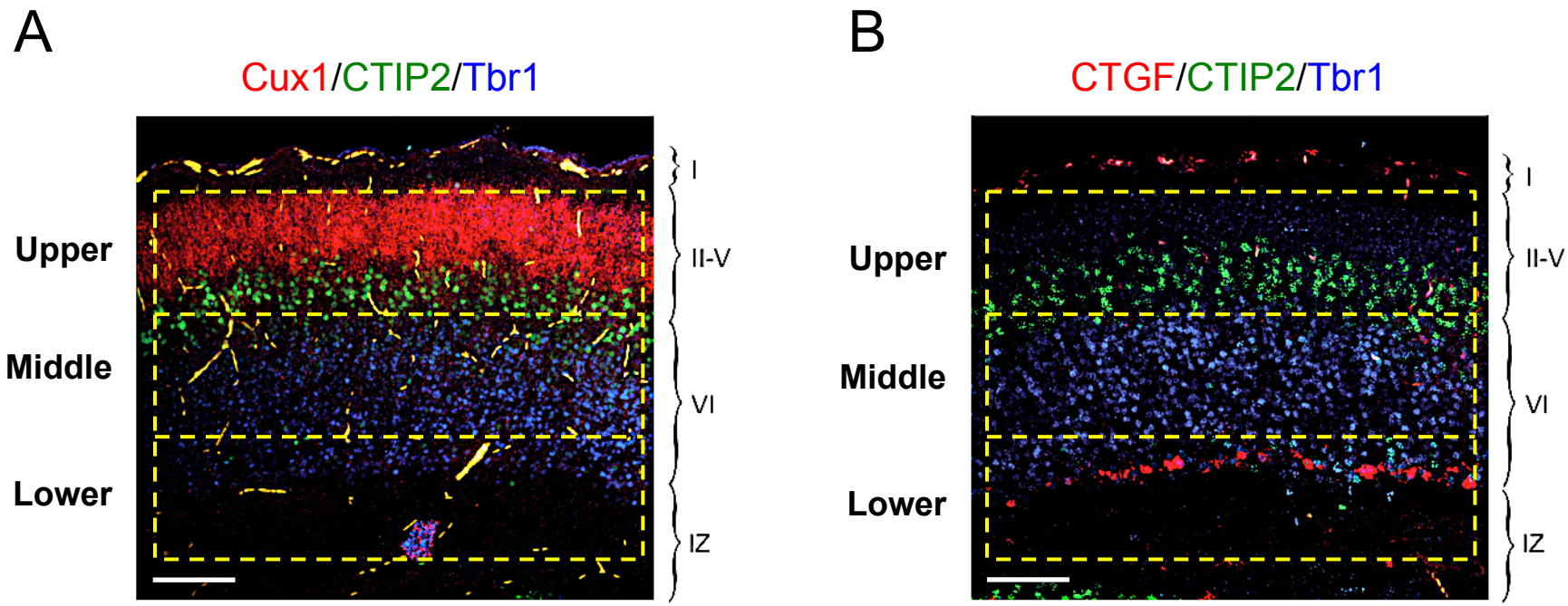
A
Cux1/CTIP2/Tbr1
Upper
Middle
Lower
I
II-V
VI
IZ
B
CTGF/CTIP2/Tbr1
Upper
Middle
Lower
I
II-V
VI
IZ

Fig. 1S5

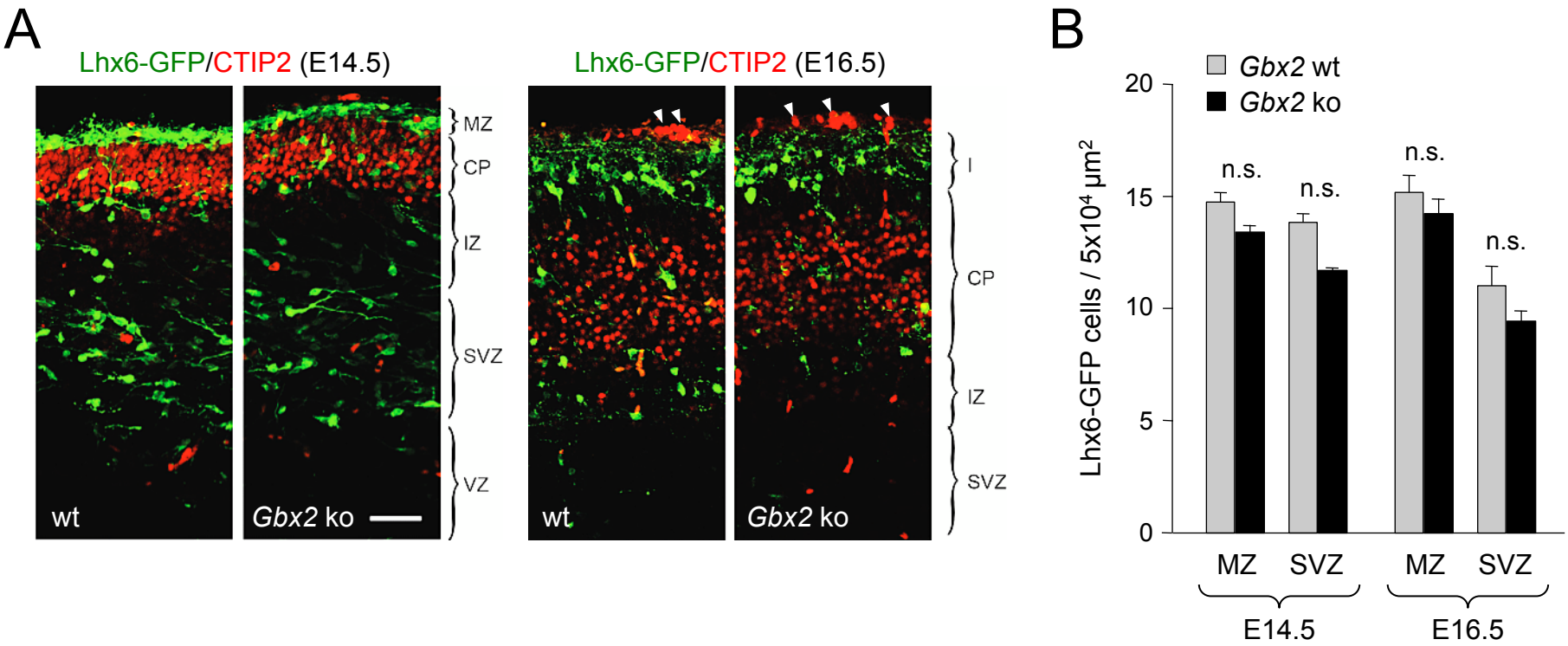
A
Lhx6-GFP/CTIP2 (E14.5)
Lhx6-GFP/CTIP2 (E16.5)
MZ
CP
IZ
SVZ
VZ
I
wt
Gbx2 ko
B
Gbx2 wt
Gbx2 ko
Lhx6-GFP cells / 5x10⁴ µm²
20
15
10
5
0
n.s.
MZ
SVZ
E14.5
E16.5

Fig. 1S6

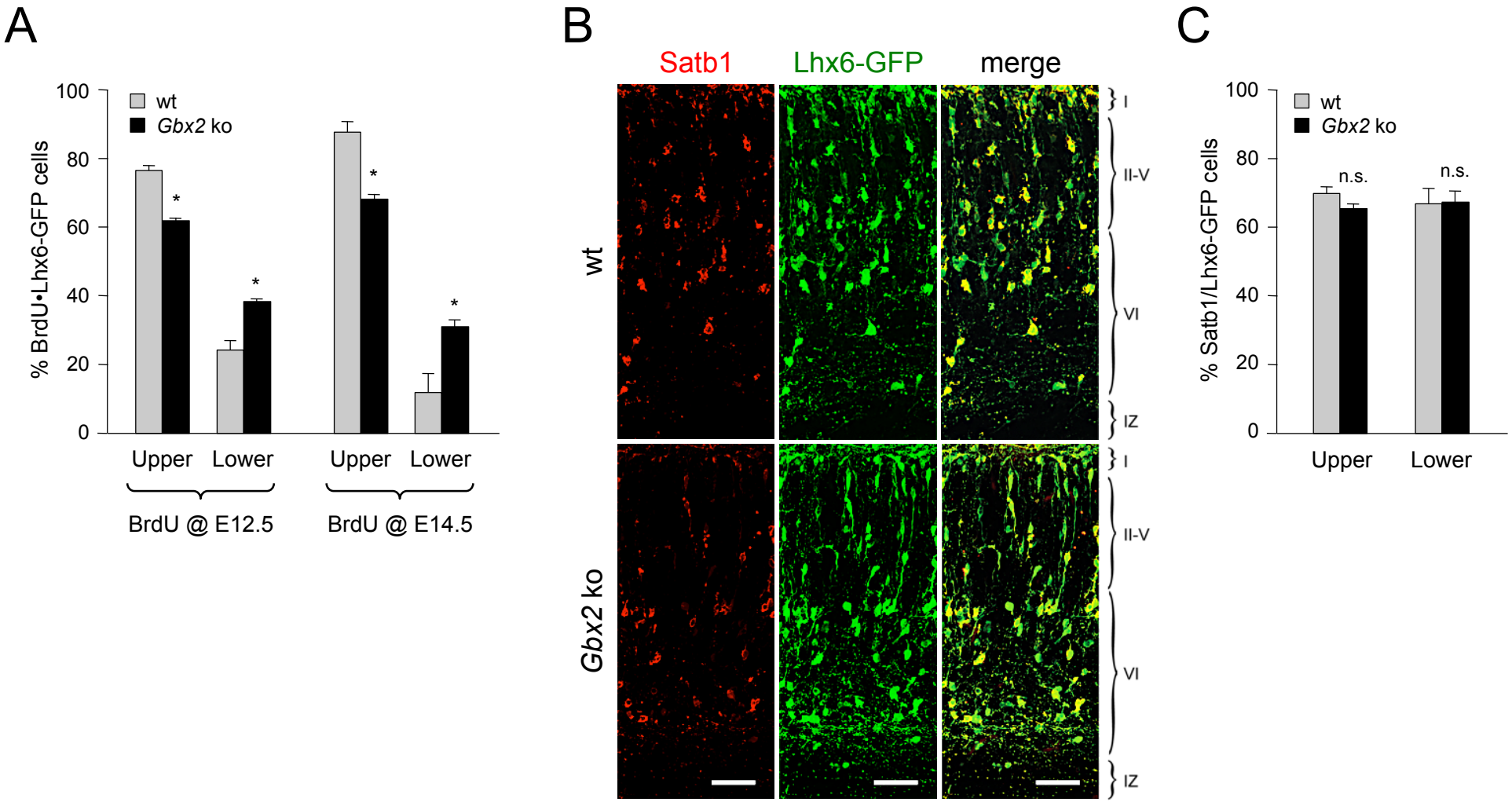
A
100
80
60
40
20
0
% BrdU•Lhx6-GFP cells
wt
Gbx2 ko
*
Upper
Lower
Upper
Lower
BrdU @ E12.5
BrdU @ E14.5
B
Satb1
Lhx6-GFP
merge
wt
Gbx2 ko
I
II-V
VI
IZ
C
% Satb1/Lhx6-GFP cells
n.s.

Fig. 2S1

A

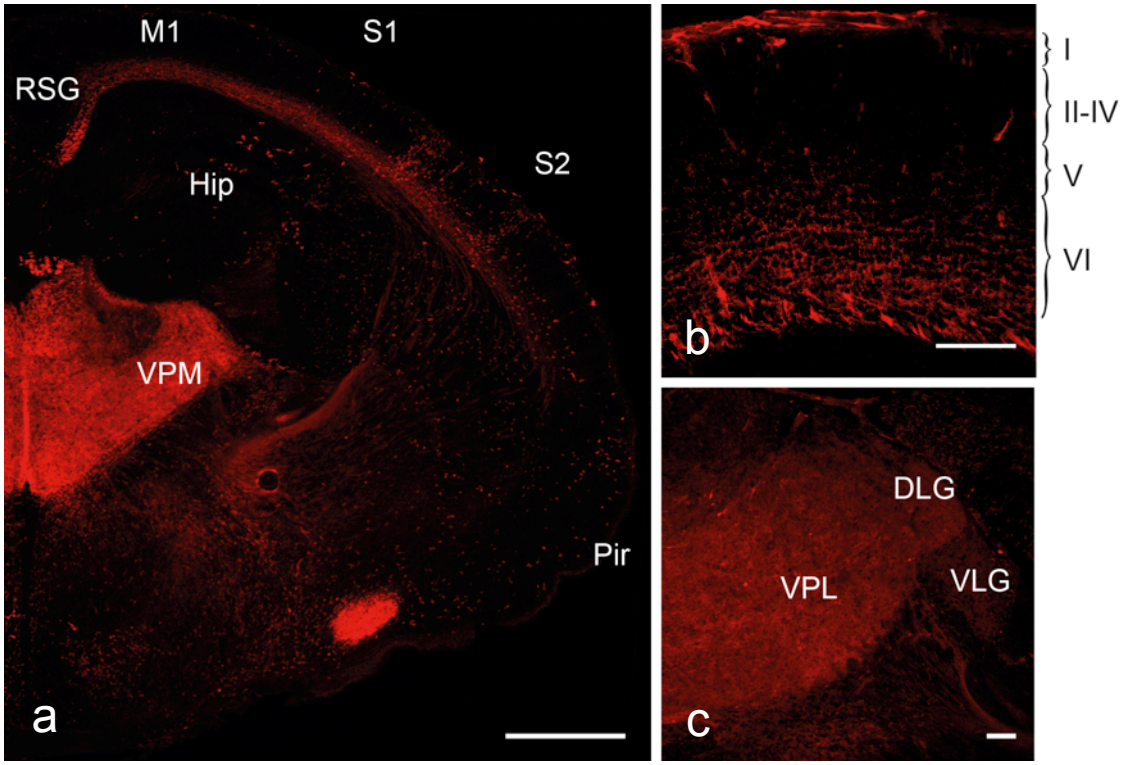
M1
S1
RSG
Hip
S2
VPM
Pir
a
b
I
II-IV
V
VI
DLG
VPL
VLG
c

B

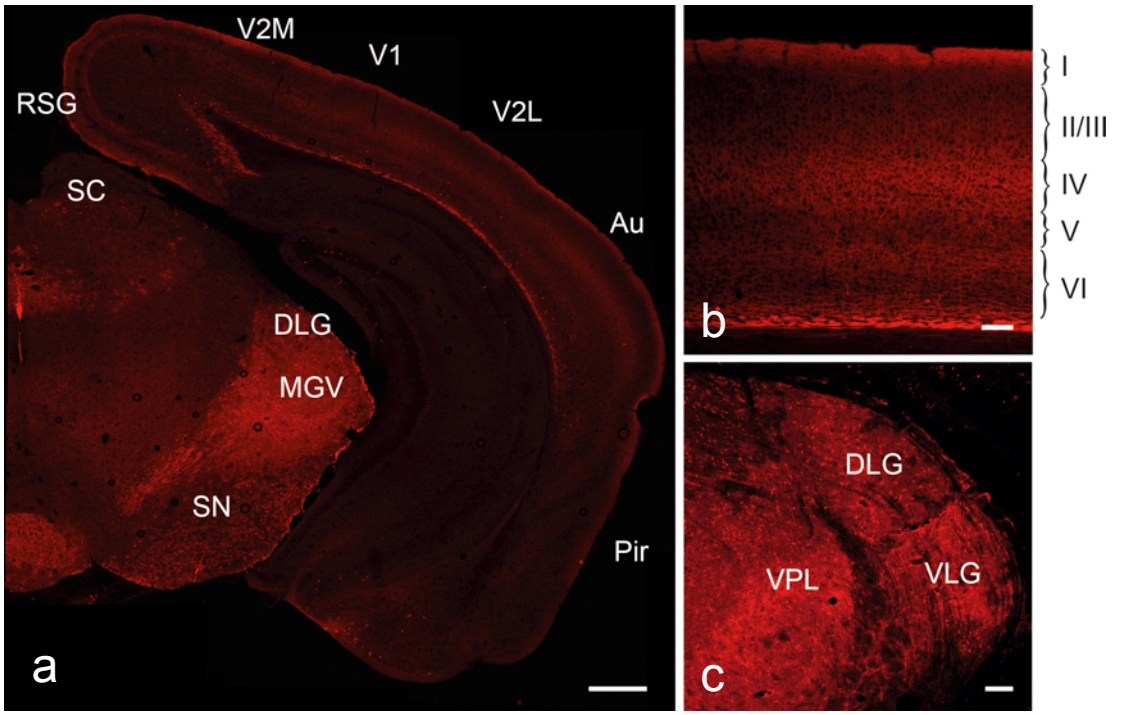
V2M
V1
RSG
V2L
SC
Au
DLG
MGV
SN
Pir
a
b
I
II/III
IV
V
VI
DLG
VPL
VLG
c

Fig. 2S2

A

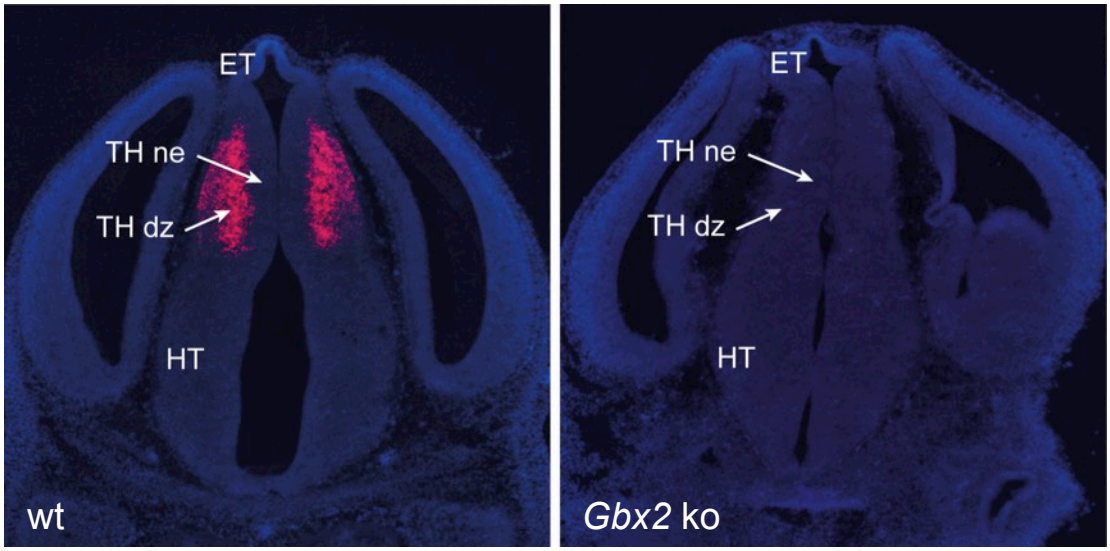
ET
TH ne
TH dz
HT
wt
ET
TH ne
TH dz
HT
Gbx2 ko

B

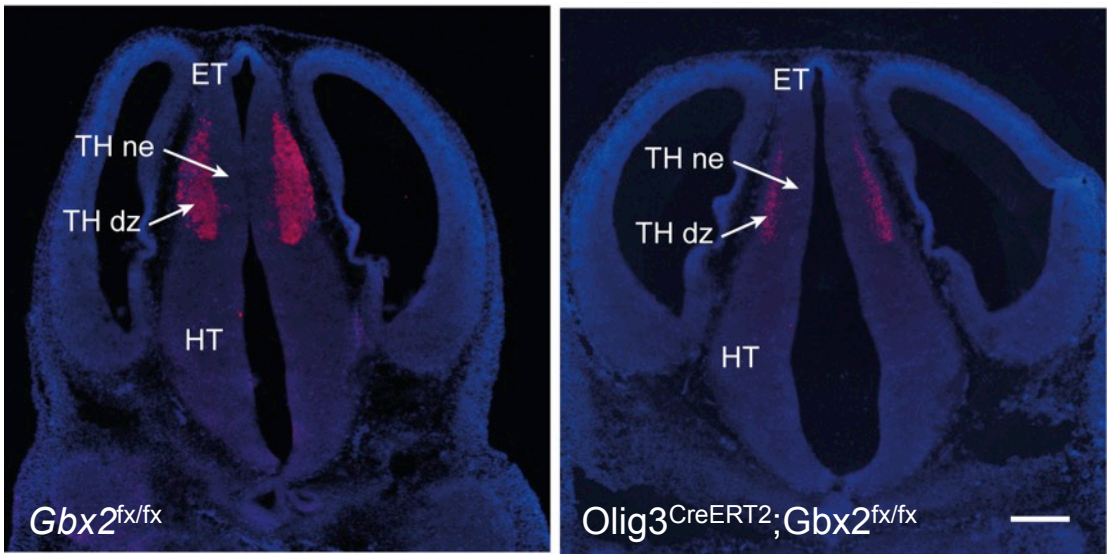
ET
TH ne
TH dz
HT
Gbx2$^{fx/fx}$
ET
TH ne
TH dz
HT
Olig3^{CreERT2};Gbx2$^{fx/fx}$

Fig. 2S3

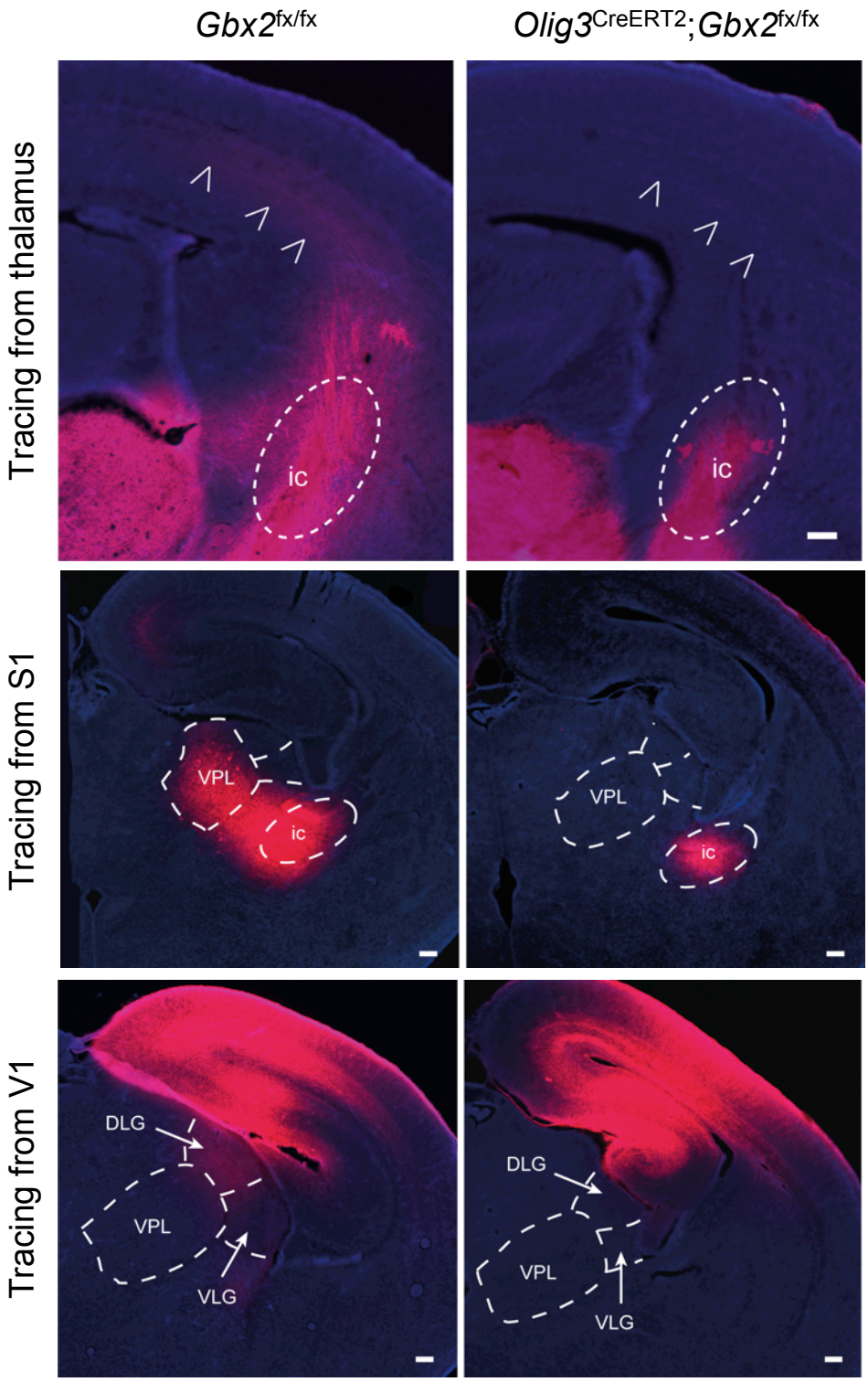
Gbx2fx/fx
Olig3CreERT2;Gbx2fx/fx
Tracing from thalamus
ic
ic
Tracing from S1
VPL
ic
VPL
ic
Tracing from V1
DLG
VPL
VLG
DLG
VPL
VLG

Fig. 2S4

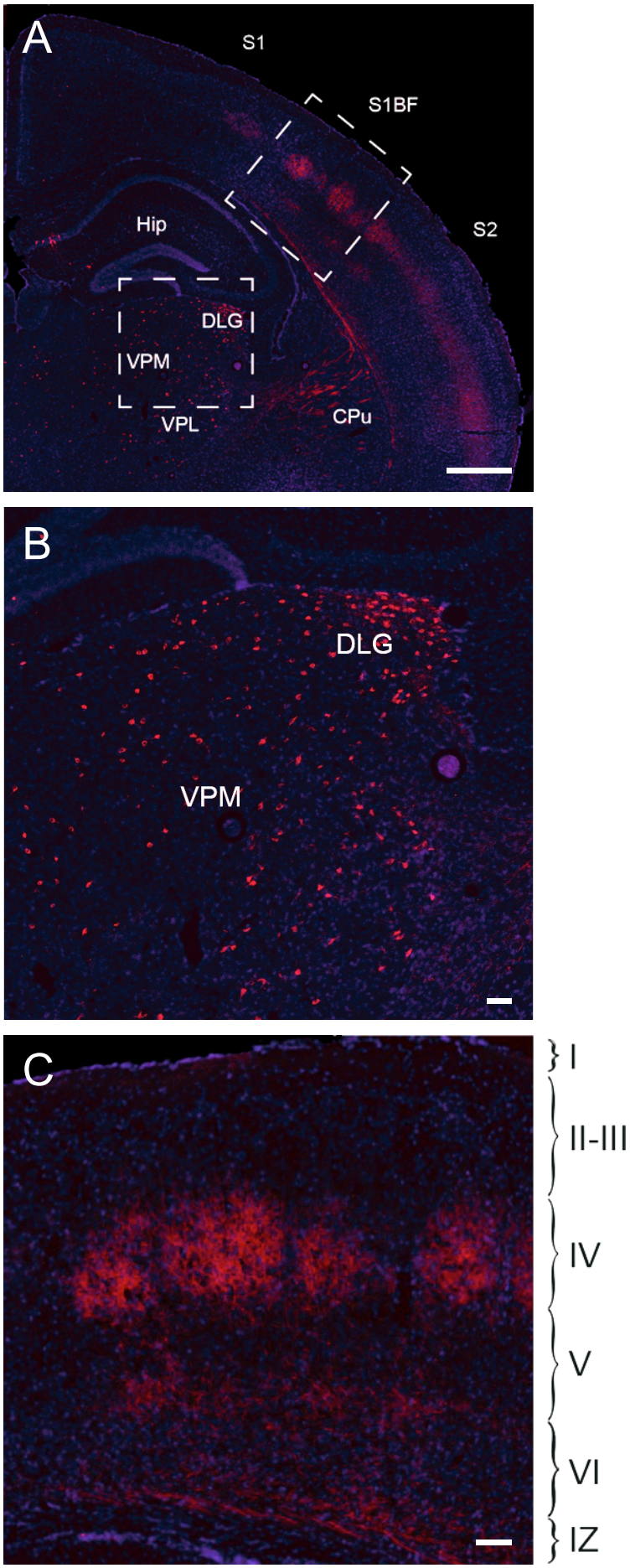

Fig. 6S1

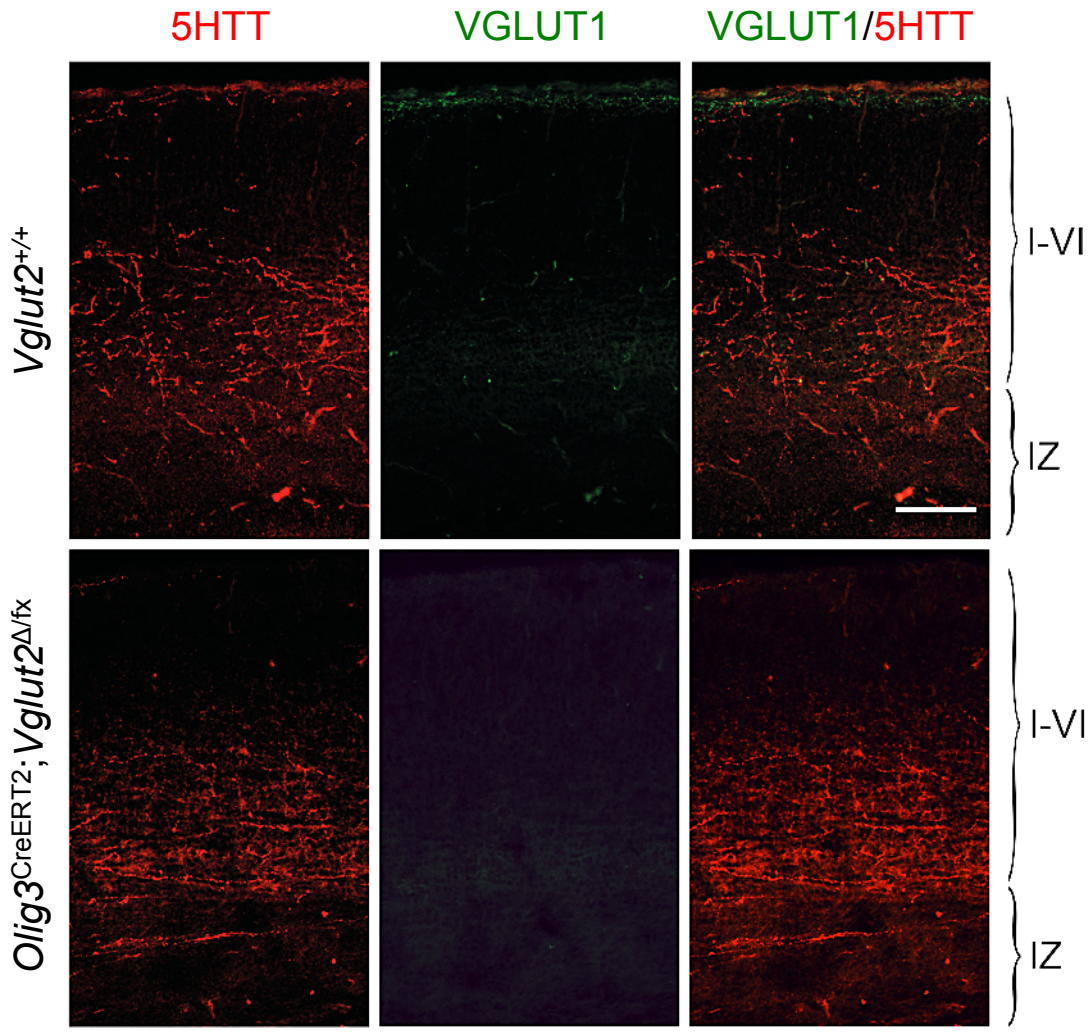
5HTT
VGLUT1
VGLUT1/5HTT
Vglut2+/+
Olig3CreERT2;Vglut2Δ/fx
I-VI
IZ
I-VI
IZ

Fig. 7S1

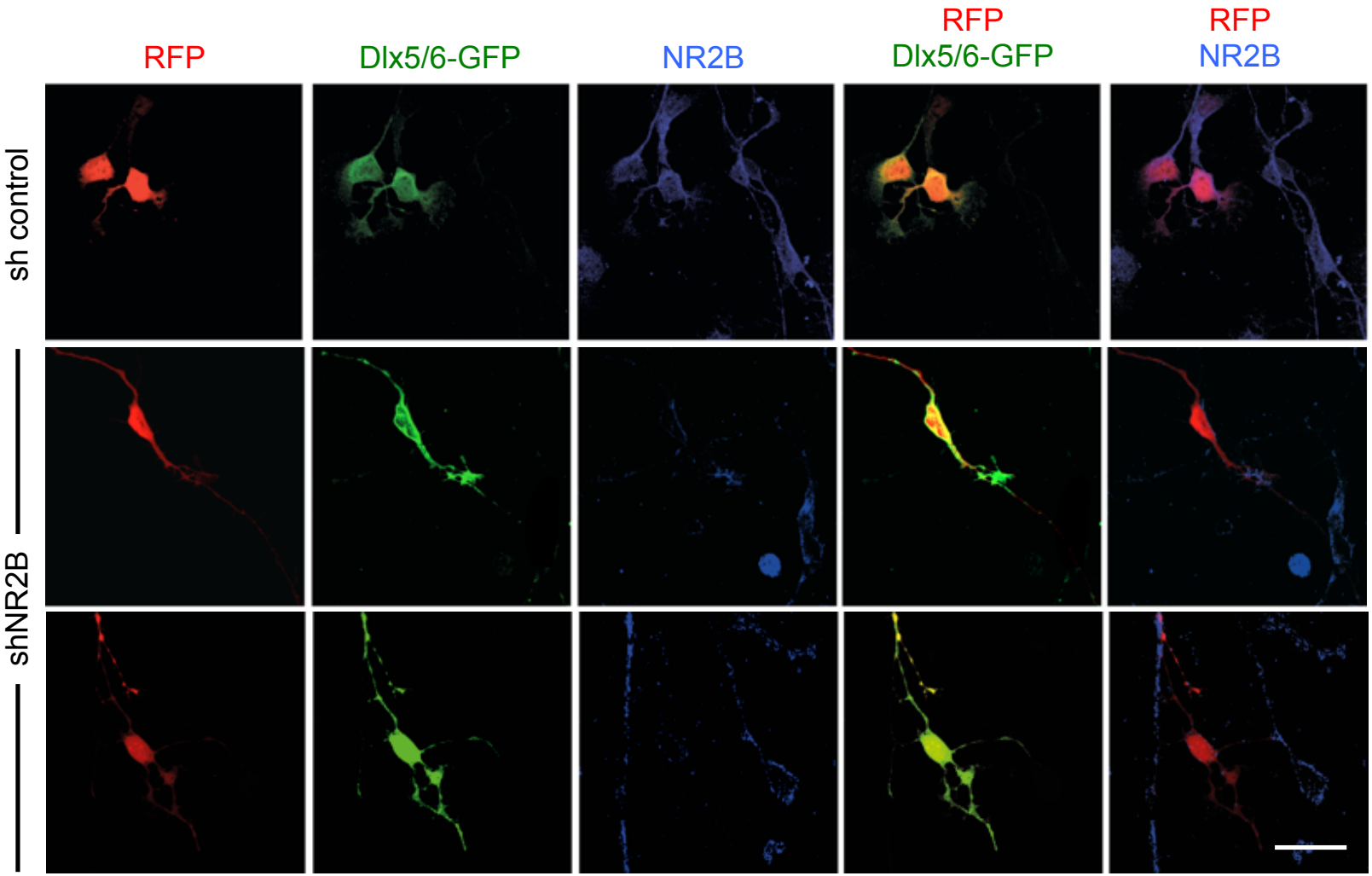

Fig. 9S1

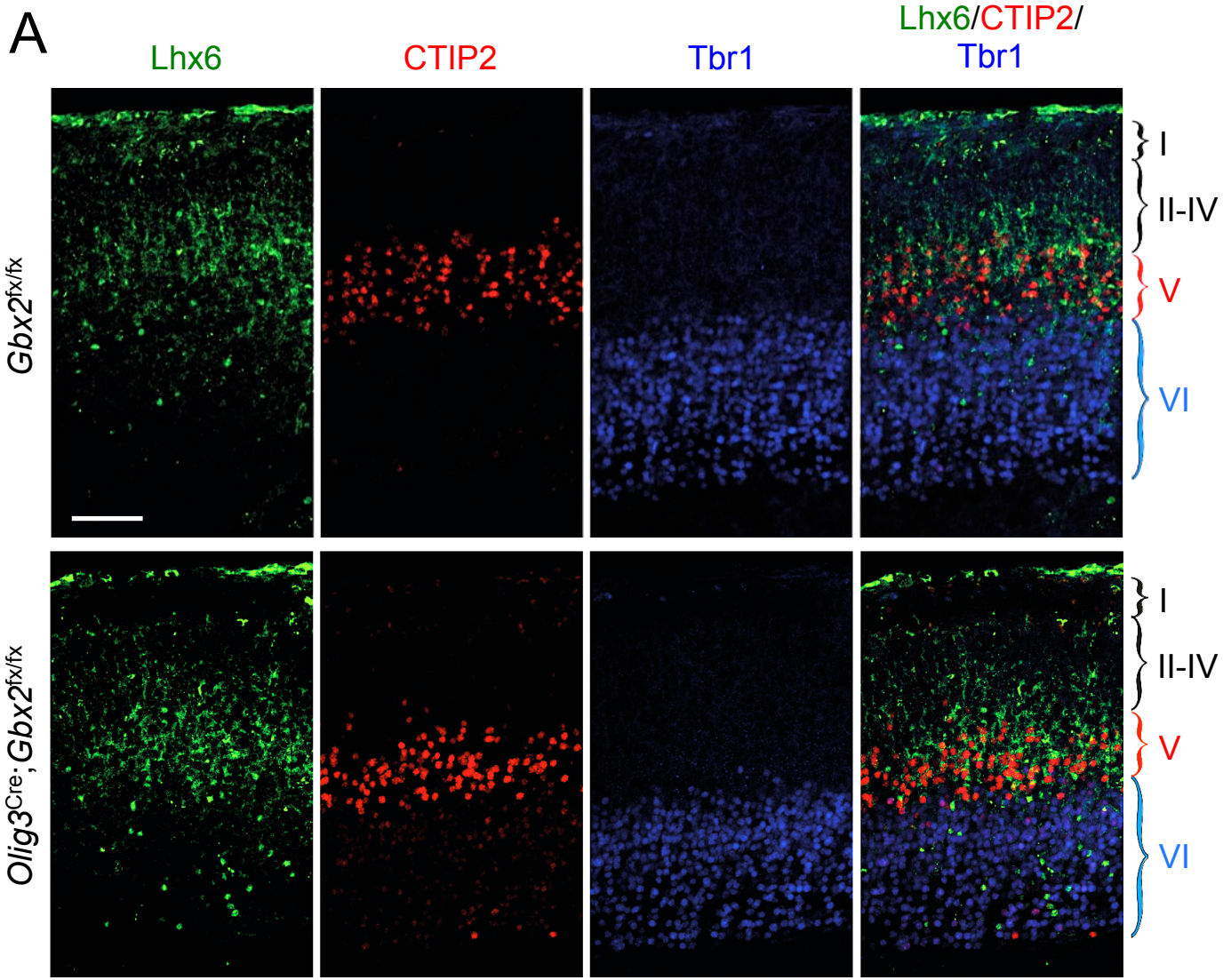
A
Lhx6
CTIP2
Tbr1
Lhx6/CTIP2/
Tbr1
Gbx2fx/fx
Olig3Cre;Gbx2fx/fx
I
II-IV
V
VI

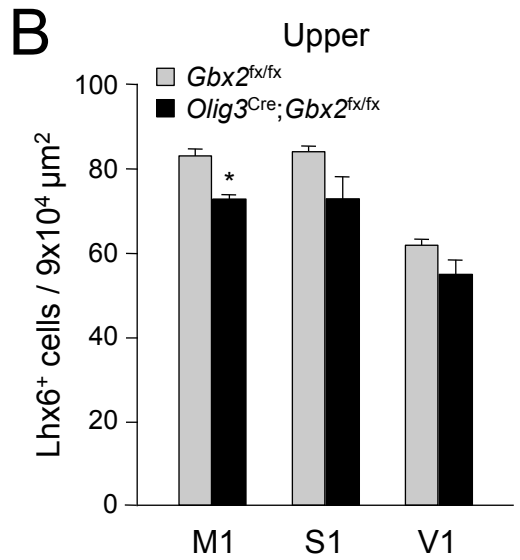
B
Upper
Gbx2fx/fx
Olig3Cre;Gbx2fx/fx
Lhx6+ cells / 9x10^4 µm^2
100
80
60
40
20
0
*
M1
S1
V1

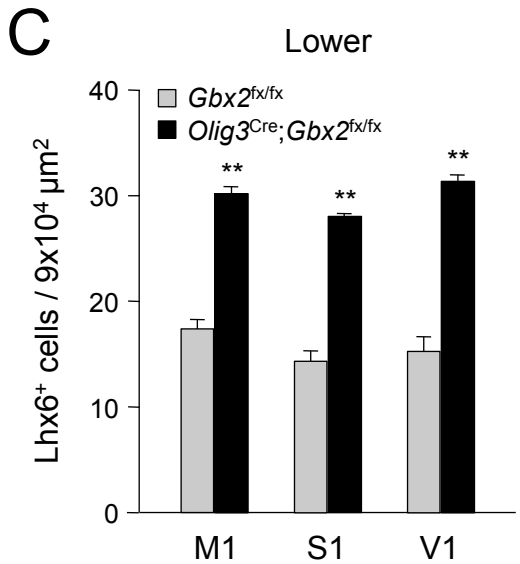
C
Lower
Gbx2fx/fx
Olig3Cre;Gbx2fx/fx
Lhx6+ cells / 9x10^4 µm^2
40
30
20
10
0
**
**
**
M1
S1
V1